

CONNECTION BETWEEN ACCRETION DISK AND SUPERLUMINAL RADIO JETS AND THE ROLE OF RADIO PLATEAU STATE IN GRS 1915+105

J. S. YADAV¹

Tata Institute of Fundamental Research, Homi Bhabha Road, Mumbai-400005, India

Accepted for publication in ApJ; March, 2006

ABSTRACT

We investigate the association between the accretion disk during radio plateau state and the following superluminal relativistic radio jets with peak intensity varies from 200 mJy to 1000 mJy observed over a period of five years and present the evidences of direct accretion disc-jet connection in microquasar GRS 1915+105. We have analysed RXTE PCA/HEXTE X-ray data and have found that the accretion rate, \dot{m}_{accr} , as inferred from the X-ray flux, is very high during the radio plateaux. We suggest that the accretion disk during the radio plateaux always associated with radiation-driven wind which is manifested in the form of enhanced absorption column density for X-ray and the depleted IR emission. We find that the wind density increases with the accretion disk luminosity during the radio plateaux. The wind density is similar to the density of the warm absorber proposed in extragalactic AGNs and Quasars. We suggest a simple model for the origin of superluminal relativistic jets. Finally, We discuss the implications of this work for galactic microquasars and the extragalactic AGNs and Quasars.

Subject headings: accretion, accretion disk – X-rays –black hole physics – quasars –stars: individual (GRS 1915+105)

1. INTRODUCTION

Large superluminal outflows/jets which appear to move faster than light are widely studied in active galactic nuclei (AGN) & quasars, yet remain poorly understood (first AGN was discovered in 1943 by Carl Seyfert!). This is due to the long time scales associated with these systems as well as the central part of these systems is usually obscured by large amount of dust. Microquasars in our galaxy are stellar mass analogs of the massive black hole systems in quasars and AGNs. Microquasars are closer, smaller and show faster variability that is easily observable. Mirabel & Rodriguez (1994) discovered first microquasar GRS 1915+105 in our galaxy with superluminal jets. The black hole mass in GRS 1915+105 is determined to be $14 \pm 4 M_{\odot}$ (Greiner, Cuby, & McCaughrean 2001). This microquasar shows exceptionally high variability in both X-rays and radio. Since 1996, rich X-ray variability of this source is observed by RXTE (Morgan, Remillard, & Greiner 1997; Munro, Morgan, & Remillard 1999) and by Indian X-ray Astronomy Experiment, IXAE (Yadav et al. 1999). Belloni et al. (2000) have classified the complex X-ray variability of GRS 1915+105 in 12 separate classes on the basis of their light curves and the color-color diagrams and suggested three basic states of this source namely low hard state, high soft state and low soft state.

The radio emission from GRS 1915+105 can be broadly classified into three types: (a) steady radio jets (radio plateau state), (b) oscillations/baby jets (discrete jets) of 20-40 min duration in infrared (IR) and radio, and (c) large superluminal radio jets. The steady radio jets of 20 – 160 mJy flux density are associated with the canonical low hard X-ray state and observed for extended durations (Munro et al. 2001; Fuchs et al. 2003). These

are optically thick compact jets of < 200 AU with velocity β of 0.1–0.4 (Dhawan, Mirabel, & Rodriguez 2000; Ribo, Dhawan, & Mirabel 2004). The radio emission is correlated with the X-ray emission as $L_{radio} \propto L_X^{0.7}$ for several different sources (Gallo, Fender, & Pooley 2003). Pooley & Fender (1997) observed radio oscillations with delayed emission at lower frequency. Simultaneous X-ray, IR and radio multi-wavelength observations provided first major step in our understanding of disk-jet interaction and suggested that the spike in X-ray coincides with the beginning of IR flare and it has self absorbed synchrotron emission associated with adiabatic expansion (Eikenberry et al. 1998; Mirabel et al. 1998). These are also compact jets with velocity $\beta \sim 1$ (Dhawan, Mirabel, & Rodriguez 2000). It is further suggested that the spike in X-ray is associated with the change of the X-ray state due to major ejection episode (Yadav 2001). This is consistent with the suggestion that it is the coronal material and not the disk material (or any other accretion flow associated with the low hard state) which is ejected prior to radio flares (Rau & Greiner 2003; Vadawale et al. 2003; Fender, Belloni, & Gallo 2004; Rothstein, Eikenberry, & Matthews 2005).

The relativistic superluminal jets with up to 1 Jy flux density have steep radio spectrum and are observed at large distances few hundred AU to 5000 AU from the core (Mirabel & Rodriguez 1994; Fender et al. 1999; Dhawan, Mirabel, & Rodriguez 2000). These radio jets are very energetic with luminosity close to the Eddington luminosity, L_{Edd} and have been observed in several sources (Fender et al. 1999; Hjellming & Rupen 1995; Wu et al. 2002; Orosz et al. 2001). Progress in our understanding of these jets specially their connection to accretion disk has been slow. A semi-quantitative model is proposed for the disk-jet coupling (Fender, Belloni, & Gallo 2004; Fender & Belloni 2004)

¹ E-mail: jsyadav@mailhost.tifr.res.in

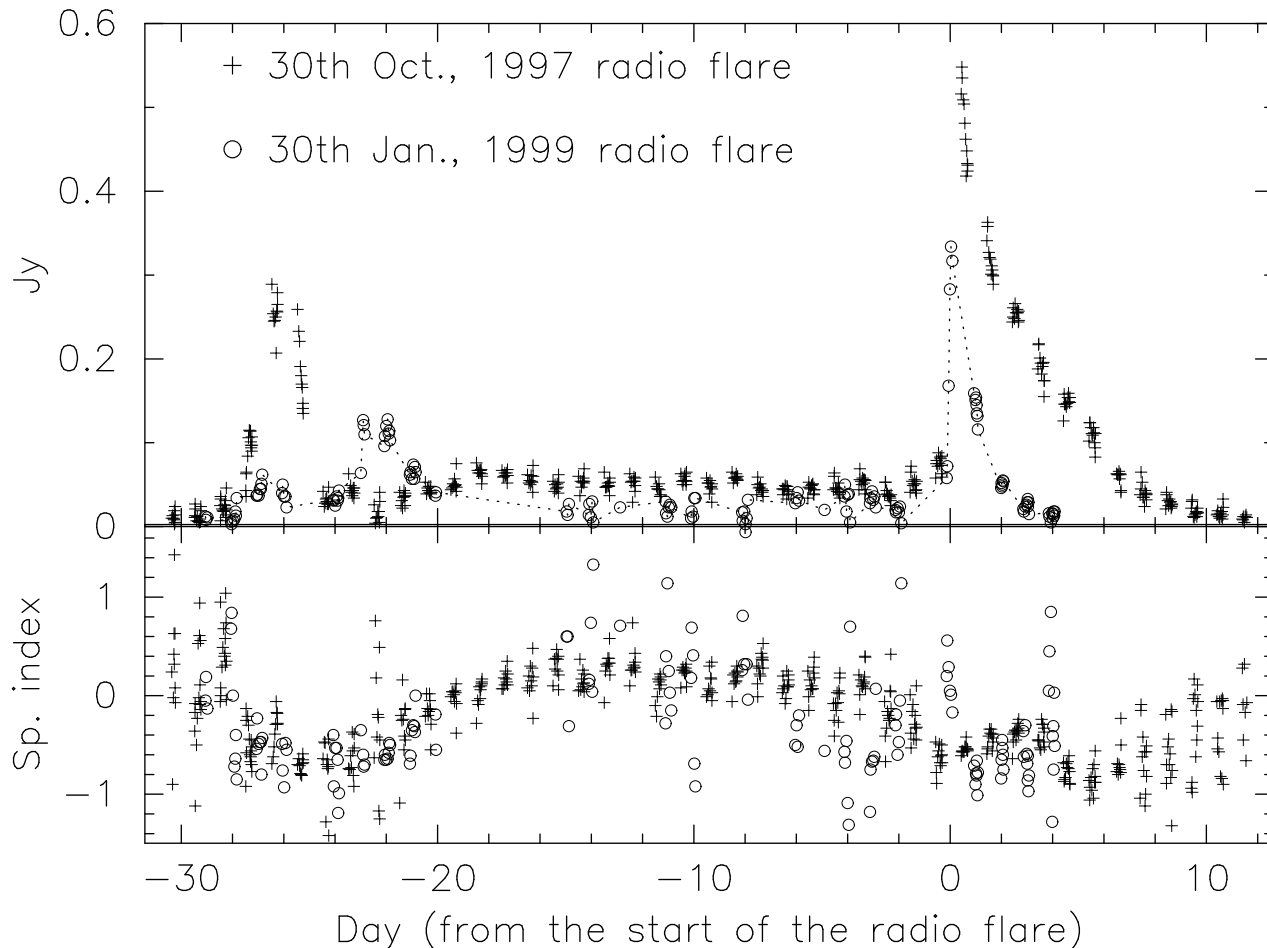


FIG. 1.— GBI 2.25 GHz radio data for 1999 January 30 (start at MJD 51204.7) and 1997 October 30 (start at MJD 50750.6) large superluminal radio flares in the top panel. Start of the flares is offset to 0. It includes preplateau flares, plateau state and the large superluminal radio flare. The dotted line connects the data points of 1999 January 30 superluminal radio flare to guide eyes. The radio spectral index is shown in the bottom panel.

which although puts all available observational details in perspective but the scope to gain new insight or new information about disk-jet interaction seems limited (Remillard 2005). The physical connection between X-ray emission and the superluminal flares has been the hardest to understand. However a general trend is emerging that the plateau states are generally followed (and perhaps preceded) by superluminal flares (Fender & Belloni 2004).

In this paper, we investigate the association of large superluminal jets with the radio plateaux. We have analysed the available RXTE PCA/HEXTE X-ray data during radio plateaux and the radio flare data from the Green Bank Interferometer (GBI). We describe our selection criterion and discuss in detail the morphology of superluminal radio flares. We present tight correlations between parameters of the accretion disk and the superluminal jets. We suggest that the accretion disk during radio plateaux always associated with radiation-driven wind and corroborate it with supporting evidences. Finally we provide a simple model for the origin of superluminal jets and discuss its implications for galactic & extragalactic radio jet sources.

2. OBSERVATIONS AND ANALYSIS

All the radio flares observed in GRS 1915+105 can be broadly put into two groups on the basis of their flux, radio spectrum and spatial distribution; (1) the superluminal flares (200–1000 mJy) which have steep radio spectra and are seen at large distances (≥ 240 AU), and (2) all other flares (5–360 mJy) which include the preplateau flares, radio oscillations & discrete flares and the steady radio flares during the plateaux. All these flares have flat radio spectra and are observed close to the compact object (< 200 AU). It is the superluminal flares which are hard to understand. The other flares in the latter group are studied in detail and understood fairly well (this is discussed in the last section). In the internal shock model for superluminal radio jets in microquasars, an exponential decay is suggested once the shock is fully developed (Kaiser, Sunyaev, & Spruit 2000). It is also found that the radio plateau is always associated with superluminal radio flare (Fender et al. 1999; Klein-Wolt et al. 2002; Vadawale et al. 2003). We searched 2.25 GHz GBI radio monitoring data during the period from 1996 December to 2000 April and selected radio plateaux and the following radio flares which decay exponentially. The preplateau radio flares do not follow exponential decay and are like the oscillations and discrete flares but closely spaced in time as described

in the next paragraph. Seven flares are found to satisfy our criteria for superluminal flares and are listed in Table 1. One more radio flare on 2001 July 16 which was observed by the Very Large Baseline Array (VLBA) and Ratan radio telescope is also added in Table 1. VLBA observations clearly showed an ejecta well separated from the core (Dhawan et al. 2003). This plus two more flares out of eight flares listed in Table 1 show moving ejecta well separated from the core (Fender et al. 1999; Dhawan, Mirabel, & Rodriguez 2000). In Table 1, rise time is the total time taken by a radio flare to rise from plateau flux to the peak flux. The gaps in the GBI data put upper limit on the rise time (< 1 day). For 340 mJy flare on 1999 January 30 the rise time is 0.25 day while for 710 mJy flare on 1998 June 3 the rise time is 0.3 day. These values are consistent with the reported values of 0.25 – 0.5 day for different microquasars (Fender, Belloni, & Gallo 2004). The decay time constant is calculated by fitting exponential decay profile to the radio flare data. The contribution due to continuous radio plateau (like flares on 1998 April 13 & 30) or any other minor flare if any is removed prior to profile fitting. The decay time constant varies from 1.12 to 4.02 days. The superluminal radio flare profile can be described as fast rise and exponential decay (FRED). Here fast rise (0.2–0.5 day) is in comparison to the decay time. For comparison the oscillations/discrete radio jets have rise and decay time in the range of 0.1 – 0.3 hr (Mirabel et al. 1998; Ishwara-Chandra, Yadav, & Pramesh Rao 2002). The integrated radio flux is calculated by integrating the fitted exponential function over duration three times the decay time constant.

The typical sequence of events for a superluminal radio flare is shown in Figure 1 for 550 mJy radio flare on 1997 October 30 (gap in GBI data at peak) and for 340 mJy radio flare on 1999 January 30. Start of the radio flares is offset to zero. A superluminal event starts with small preplateau flares followed by steady long plateau, followed by superluminal radio flares. We have described the radio plateau state and the superluminal flares in previous section. The preplateau flares are studied in detail using GMRT and RYLE radio telescope data for 2001 July 16 superluminal flare (Ishwara-Chandra, Yadav, & Pramesh Rao 2002; Yadav et al. 2003). These are discrete ejections of adiabatically expanding synchrotron clouds with flat radio emission (delayed emission at lower frequency). They are like the oscillations/discrete jets but closely spaced in time and hence produce overlapped radio flares. Radio emission at 1.4 GHz and 15 GHz supports flat radio spectrum.

We study X-ray properties during radio plateaux within the preceding week from the start of superluminal flares to avoid changes in accretion disk over the long durations of plateaux (from -7 to -2 in Figure 1). We also avoid last day of plateaux as radio data suggest rapid changes in the accretion disk. For the timing analysis, we used single-bit-mode RXTE/PCA data in the energy ranges 3.6 – 5.7 and 5.7 – 14.8 keV. Power density spectra of 256 bin light curves are generated and co-added for every 16 s. The power density spectra are normalised. We fit a model of power law + Lorentzian and have calculated quasi-periodic oscillation (QPO) frequency. We show in Figure 2 the power density spectra in 0.09 – 9 Hz

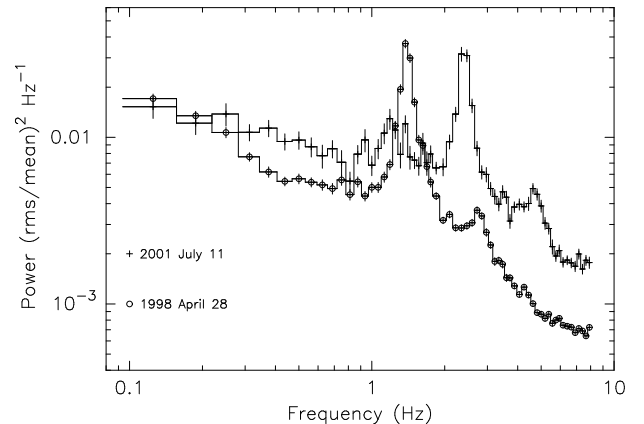


FIG. 2.— Normalised power density spectra in 0.09 – 9 Hz frequency range observed on 1998 April 28 and 2001 July 11. Strong QPOs are seen at 1.4 Hz and 2.4 Hz in PDS observed on 1998 April 28 and 2001 July 11 respectively. The first harmonics are also visible in spectra.

frequency range observed on 1998 April 28 and 2001 July 11. Strong QPOs are seen at 1.4 Hz and 2.4 Hz in PDS observed on 1998 April 28 and 2001 July 11 respectively. The first harmonics are also visible in the spectra. For spectral analysis, we used PCA standard-2 data (3 – 35 keV) and cluster 0 data from HEXTE (20 – 150 keV). We added 0.5% systematic error in PCA data. Standard procedures for data reduction, response matrix and background estimation are followed using HEASOFT (ver 5.2). Munro, Morgan, & Remillard (1999) have shown that a spectral fit using sum of multicolor disk blackbody, power law and a gaussian line during plateaux results high values of the inner disk temperature (≥ 3 keV) and unrealistic accretion disk radius (≤ 2 km). Fuchs et al. (2003) also drew similar conclusion while analysing X-ray properties during a plateau state using INTEGRAL and RXTE data. Rau & Greiner (2003) analysed large sample of RXTE observations belonging to radio plateaux using multicolor disk-blackbody + power law spectrum reflected from the accretion disk. This model adequately describes the X-ray spectra of all the observations, but it yields extremely high values of reflection parameter inconsistent with other measurements.

A spectral model of simple power law with multicolor disk-blackbody and a gaussian provides reasonable values of temperature and inner radius of the disk if the energy spectrum is disk dominated as is the case during class β (Migliari & Belloni 2003). During the plateaux, the source is in very high luminosity state (VHS) with power index $\Gamma > 2$. The spectrum is dominated by the Compton scattered emission ($\geq 85\%$) rather than the disk. The comptonised emission has a complex spectrum shape showing features from both thermal and non-thermal electrons (Chris & Kubota 2005). It suggests the presence of an optically thick inner disk corona which drains energy from the disk and reduces the disk temperature. The presence of QPO in 1.4 – 2.6 Hz frequency range is consistent with the large corona (see Table 1). This will require additional component in the spectral model during the plateaux. A three component model (multicolor disk-blackbody + power law + a comptonised component (CompTT)) with a gaussian line at 6.4 keV

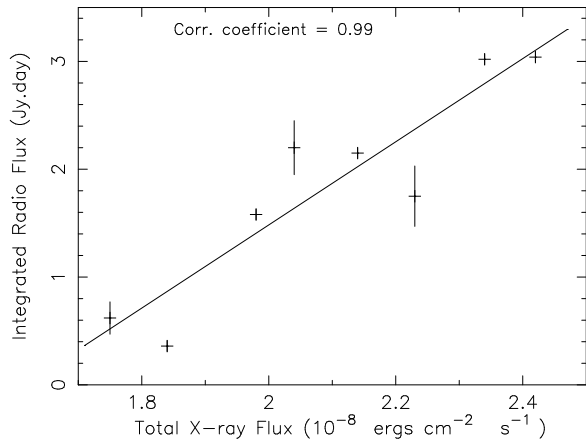


FIG. 3.— Correlation between the total 3-150 keV X-ray flux from spectral analysis of RXTE PCA/HEXTE X-ray data during preflare plateau state and the integrated flux of the superluminal radio flare. The solid line is the linear fit to the data points.

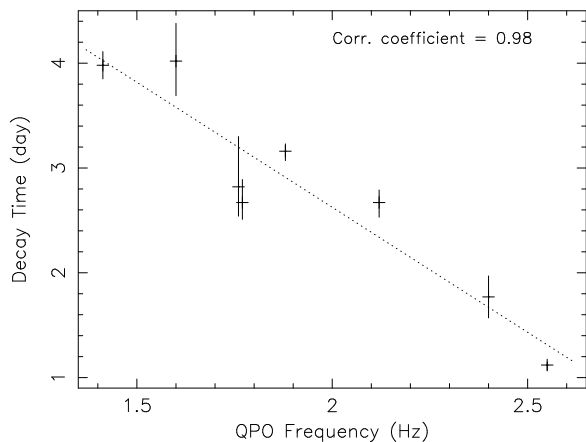


FIG. 4.— Correlation between the quasi-periodic oscillation (QPO) frequency from timing analysis of RXTE/PCA X-ray data during preflare plateau state and the decay time constant of the superluminal radio flare. The dotted line is the linear fit to the data.

is reported to provide more realistic values of the inner disk temperature and the disk radius (Rao et al. 2000; Vadawale et al. 2003). We have used this model for our X-ray spectral analysis during plateaux listed in Table 1. The absorption column density, N_H is kept as free parameter. The integrated X-ray flux for energy range 3 – 150 keV and the derived values of N_H are listed in Table 1. The other best-fit X-ray spectral parameters are given in Table 2 along with the flux of the individual spectral components. The χ^2_ν of our spectral fits falls in the range 0.81 to 1.4 (for dof 74-94). The spectrum is dominated by the Compton scattering emission and the contribution from the disk is limited to less than 13%.

3. RESULTS AND DISCUSSION

It is widely believed that the coronal material (and not the disk material) is ejected prior to radio flares as discussed earlier. It is consistent with the observation that radio flares are observed during transition from the low hard state to the high soft state but never observed during opposite transition (Klein-Wolt et al. 2002). All the radio flares observed close to the core

in GRS 1915+105 can be further subdivided into two groups on the basis of associated change observed in the accretion disk; (1) the persistent radio flares during the plateaux with steady accretion disk (no change associated with radio flares) and, (2) all other radio flares which accompany clear change in the accretion disk. In the former case, inflow and outflow in the accretion disk are in equilibrium. Both the accretion disk and the radio flare are in steady state and radio emission is tightly correlated with the X-ray luminosity as discussed above. In latter case, the hard X-ray component (Compton component) is either partly or completely affected. The large changes will result state transition (Rothstein, Eikenberry, & Matthews 2005; Rau & Greiner 2003; Yadav 2001). The accretion disk may come back to its initial state after some time or may remain in the new state for a longer duration. If the accretion disk is in some periodic state like in class β or θ (Belloni et al. 2000), it produces IR and radio oscillations. Eikenberry et al. (1998) suggested that the spike in X-ray during the class β is related to mass ejection and the ejected matter decouples from the accretion disk. It is further shown that the intensity of these IR and radio jets increases with the X-ray hardness ratio during the low hard state preceding the spike (Yadav 2001). For these oscillations and the preplateau radio flares, all the available experimental data of time delay in emission at lower frequencies can be adequately explained using adiabatically expanding synchrotron emitting cloud ejected from the accretion disk (Ishwara-Chandra, Yadav, & Pramesh Rao 2002). These results suggests that the ejected matter behaves like an adiabatically expanding synchrotron cloud which has been decoupled from the accretion disk.

Muno et al. (2001) have shown that radio emission during large superluminal flares is decoupled from the accretion disk. This view is further strengthened by the fact that superluminal flares appear at distances few hundred AU from the core (Fender et al. 1999; Dhawan, Mirabel, & Rodriguez 2000). Fender et al. (1999) have observed superluminal flares after a radio plateau state. To investigate the association of superluminal flares with plateaux, we plot in Figure 3 the total 3–150 keV X-ray flux during the preceding plateau vs the integrated radio flux of the superluminal flare. We derive a correlation coefficient of 0.99 suggesting a strong connection between the total X-ray flux during the preceding plateau state and the integrated radio flux of the superluminal flare. We also find strong correlation between ASM count rate vs plateau radio flux and ASM count rate vs the integrated radio flux as discussed by Vadawale et al. (2003) (not shown here). In Figure 4, we plot QPO frequency from our timing analysis of X-ray data during the plateau state as a function of decay time constant of the following superluminal radio flare. It again shows a tight correlation with correlation coefficient of 0.98. The remarkable feature of our findings here is that the parameters calculated using completely independent spectral and timing analysis bring out clear connection between the accretion disk during the plateau state and the following superluminal radio flare.

In the last column of Table 1, we give calculated value of N_H which ranges from 10×10^{22} to $15 \times 10^{22} \text{ cm}^{-2}$. These values are higher than

commonly used $N_H \sim 5 - 6 \times 10^{22} \text{ cm}^{-2}$ for spectral analysis of GRS 1915+105 by several authors (Belloni et al. 1997; Munro, Morgan, & Remillard 1999; Yadav 2001; Rau & Greiner 2003). Radio emission from atomic hydrogen & molecular hydrogen together puts line-of-sight column density $\geq 3 \times 10^{22} \text{ cm}^{-2}$ (Dickey & Lockman 1990; Dame, Hartmann, & Thaddeus 2001). Belloni et al. (2000) found for the first time evidences for a variable N_H during the plateau (class χ_1 & χ_3) and suggested presence of a large intrinsic absorber. The value of N_H estimated to be $6 \times 10^{22} \text{ cm}^{-2}$ for plateau state while for non-plateau low hard state, it is found to be $2 \times 10^{22} \text{ cm}^{-2}$. Lee et al. (2002) have analysed CHANDRA & RXTE X-ray data during a radio plateau state with GBI radio flux of 20 mJy at 2.25 GHz on 2000 April 24. The total 2–25 keV X-ray flux is $1.89 \times 10^{-8} \text{ ergs cm}^{-2} \text{ s}^{-1}$. These plateau conditions are identical (in radio & X-ray flux) to the one preceding the superluminal flare on 2001 July 16 listed in Table 1. The K absorption edges from Fe, Si and others are detected in CHANDRA data which suggests the presence of a warm absorber in the vicinity of accretion disk. The N_H derived from Fe absorption edge is found to be $9.3_{-1.3}^{+1.6} \times 10^{22} \text{ cm}^{-2}$ for solar abundances which is in agreement with our calculated value of $N_H \sim 10.6_{-0.4}^{+0.8} \times 10^{22} \text{ cm}^{-2}$ for the superluminal flare on 2001 July 16 (see Figure 5). The lower limit of bolometric luminosity $L_{bol} \sim L_X = 6.4 \times 10^{38} \text{ ergs s}^{-1}$ which is 0.35 of Eddington Luminosity, L_{Edd} for a black hole of mass $14 M_\odot$ (Lee et al. 2002). The corresponding lower limit of bolometric luminosity for the X-ray flux listed in Table 1 falls in the range of 0.35 – 0.48 of L_{Edd} . Lee et al. (2002) have suggested wind from the accretion disk as the source of observed enhanced N_H . One can define wind (spherical) mass outflow rate, $\dot{m}_{wind} \sim 4\pi r^2 \rho v (\Omega/4\pi) \sim 9.5 \times 10^{18} (\Omega/4\pi) \text{ g s}^{-1}$ where r is the radius (10^{11} cm), ρ is the density of the absorbing material and v is the wind velocity (100 km s^{-1}). The accretion rate, $\dot{m}_{accr} = L_{bol}/(\eta c^2) \geq L_X/(\eta c^2) \sim 7.1 \times 10^{18} \text{ g s}^{-1}$ where the efficiency $\eta \sim 0.1$. It shows that as covering fraction ($\Omega/4\pi$) approaches unity, the wind outflow rate, \dot{m}_{wind} is comparable to the \dot{m}_{accr} . During the low hard state, the efficiency of compact persistent radio jets is estimated to be $\sim 5\%$ (Fender 2001; Fender, Belloni, & Gallo 2004). In this case, losses due to non-radiative process (like adiabatic expansion) are likely to dominate. Our estimate of \dot{m}_{wind} above suggests that the major part of accretion energy goes to the wind during the plateaux. When GRS 1915+105 is accreting near L_{Edd} , the presence of a radiation-driven wind is always expected and the wind density should be a strong function of the disk luminosity. Our derived values of N_H show strong dependence on observed total X-ray flux with correlation coefficient of 0.995 which is shown in Figure 5. The dotted line is a linear fit to our data (plus sign with error bars). The open circle with error bar shows the value derived from CHANDRA and RXTE data as discussed above which is in agreement with our data within error bars. Kotani et al. (2000) have estimated $N_H \sim 10^{24}$ from ASCA data. Our estimates of N_H falls between these two values.

The best-fit X-ray spectral parameters are given in Ta-

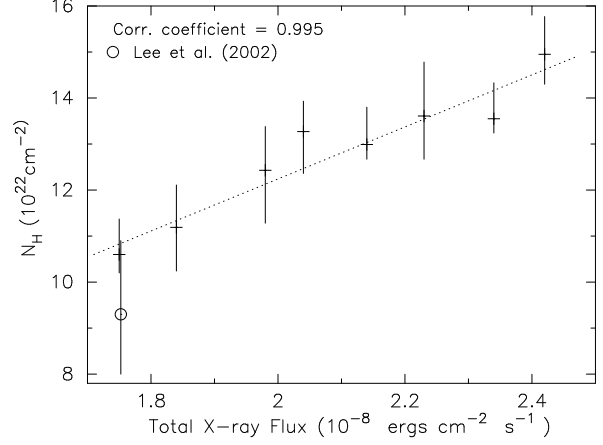


FIG. 5.— Correlation between the total 3–150 keV X-ray flux and the absorption column density, N_H (plus sign with error bars). The dotted line is the linear fit to our data. The open circle (with error bar) is the derived N_H for the solar abundances from CHANDRA and RXTE X-ray data by Lee et al. (2002) during a plateau state with 20 mJy radio flux which is similar to the one observed during the plateau preceding the superluminal flare on 2001 July 16 (for detail see text).

ble 2 along with the flux of individual spectral components. The spectrum is dominated by the Compton scattering emission and the contribution from the disk is limited to $< 13\%$. The inner-disk temperature (kT_{in}) and the plasma temperature (kT_e) are ~ 0.5 and $4\text{--}7 \text{ keV}$ respectively which are in acceptable range (Vadawale et al. 2003). The derived inner-disk radii (R_{in}) are in the physically plausible range of $(10\text{--}25) R_g$ for $14 \pm 4 M_\odot$ black hole. As the total X-ray flux rises from $1.75 \times 10^{-8} \text{ ergs cm}^{-2} \text{ s}^{-1}$ to $2.42 \times 10^{-8} \text{ ergs cm}^{-2} \text{ s}^{-1}$, the major part of it (close to 80%) goes to the COMPTT component which shows strong correlation with N_H (this is analogous to the solar wind originating from the dense solar corona). Our spectral model does not overestimate the value of N_H . Vadawale et al. (2003) have analysed preplateau data of 2001 June 30 when source was in the low hard state (non-plateau, plateau started on 2001 July 03) and estimated $N_H \sim 1.65 \times 10^{22} \text{ cm}^{-2}$ which is close to the value estimated by Belloni et al. (2000) for non-plateau low hard state. We have also studied the X-ray class β in GRS 1915+105 using this spectral model which results $N_H \sim 7 \times 10^{22} \text{ cm}^{-2}$ for χ^2_ν close to one (Yadav 2006). Similar N_H has been used earlier for spectral studies of the X-ray class β (Migliari & Belloni 2003).

Our calculated power density spectra shown in Figure 2 also independently lend support to the presence of wind during the plateau state. In the high soft state, the PDS is a featureless power law of $dP/d\nu \propto \nu^{-\alpha}$ where α is $\sim 4/3$. On the other hand, the low hard state is dominated by the Compton scattering photon emission and the PDS develops bandwidth limited noise, a flat-shoulder with a QPO at 1–4 Hz (Rao, Yadav, & Paul 2000; Meier 2005). As the power of corona (Compton scattered emission) increases, the power in the PDS increases at higher frequency ($\nu \geq 0.1 \text{ Hz}$) and the QPO frequency decreases. Figure 2 shows PDS spectra observed on 2001 July 11 and 1998 April 28. The Compton scattered flux increases from $1.5 \times 10^{-8} \text{ ergs cm}^{-2} \text{ s}^{-1}$ on 2001 July 11 to $1.9 \times 10^{-8} \text{ ergs cm}^{-2} \text{ s}^{-1}$ on 1998 April

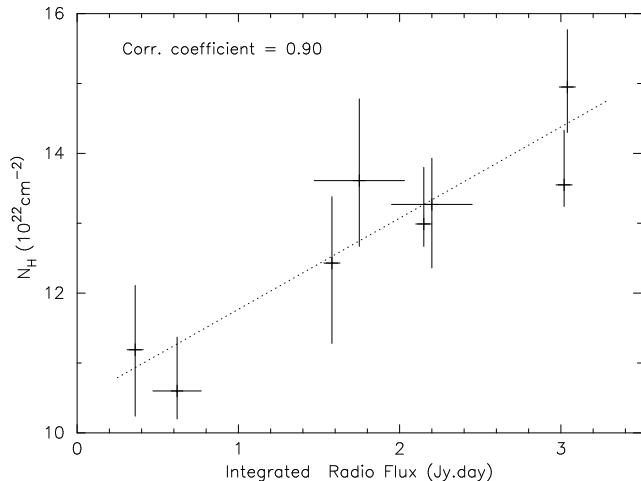


FIG. 6.— Correlation between the integrated radio flux of the superluminal radio flares and the absorption column density, N_H calculated from X-ray spectral analysis of RXTE PCA/HEXTE data during preflare plateau state. The dotted line is a linear fit to the data.

28 while observed QPO frequency decreases from 2.4 Hz on 2001 July 11 to 1.4 Hz on 1998 April 28. It is clear from Figure 2 that power at $\nu > 0.2$ Hz is less in the PDS observed on 1998 April 28 than that observed on 2001 July 11. The fast variability is suppressed by photon scattering in the enhanced wind on 1998 April 28 and hence reducing the power in the PDS at higher frequencies. Shaposhnikov & Titarchuk (2006) have discussed the decrease in the PDS power observed in Cyg X-1 at higher frequency ($\nu > 0.1$ Hz) as wind increases. In Cyg X-3, the PDS power in the low hard state drops to below 10^{-3} (rms/mean) 2 Hz $^{-1}$ at frequencies $\nu > 0.1$ Hz as dense wind from the companion always envelops the compact object (Yadav 2006).

Kotani et al. (2000) analysed ASCA data of two GRS 1915+105 observations in the low hard state in 1994 & 1995 and detected characteristic absorption lines which suggest large values of N_H . They have discussed radiation-driven wind from the accretion disk as the source of enhanced N_H and estimated wind terminal velocity of the order of 10^8 cm s $^{-1}$ for the values of r and L_X discussed above. They have speculated wind's role in the formation of superluminal radio jets. The spectral analysis of energy spectra during the extended low soft state requires large N_H which lends further support for the radiation-driven wind from the accretion disk (Vadawale, Rao, & Naik 2002). The evidences for a Seyfert-like warm absorber have been found in other microquasars like GRO J1655-40, GX 339-4 and XTE J1650-500 beside GRS 1915+105 (Miller et al. 2004; Ueda et al. 1998; Lee et al. 2002; Kotani et al. 2000) and superluminal flares have been observed in all these sources except XTE J1650-500. In Figure 6, we plot the integrated radio flux of superluminal flare as a function of N_H calculated from the X-ray data during the preceding plateau state. It brings out clearly the connection between the superluminal flare and the enhanced N_H with correlation coefficient of 0.90. The dotted line is a linear fit to the data. The wind density for typical one AU sphere comes out to be $\sim 10^9$ cm $^{-3}$ which is

similar to the value proposed in quasars (Elvis 2000).

The presence of a dense absorber close to the vicinity of the accretion disk should affect the IR emission during the radio plateaux. The source size of the steady compact jet during the radio plateau state varies as a function of frequency which is consistent with self-absorbed steady outflow (Dhawan, Mirabel, & Rodriguez 2000; Fuchs et al. 2003; Fender, Belloni, & Gallo 2004). It is similar to the self-absorbed discrete outflows in the case of oscillations/baby jets which produce delayed emission at lower frequencies (Mirabel et al. 1998; Eikenberry et al. 1998; Ishwara-Chandra, Yadav, & Pramesh Rao 2002; Ueda et al. 2002). In both the cases, the radio emission is flat or inverted. The IR emission during radio plateaux in GRS 1915+105 (Fuchs, Mirabel, & Claret 2003; Fuchs et al. 2003) is closer to the IR emission in Cyg X-3 where wind from the companion always envelops the compact object (Ogley, Burnell, & Fender 2001; Koch-Miramond et al. 2002).

Our results support the internal shock model for the origin of superluminal flares (Kaiser, Sunyaev, & Spruit 2000). The internal shock should form in the previously generated slowly moving wind from the accretion disk with $\beta \leq 0.01$ (Kotani et al. 2000) as the fast moving discrete jet with $\beta \sim 1$ (Dhawan, Mirabel, & Rodriguez 2000) catches up and interacts with it. Both the components; slow moving wind and fast moving jet are related to the accretion disk during plateau state and the strength & speed of these two components will determine the power of the internal shock. This aspect has been brought out clearly by the correlations presented in Figures 3, 4 & 6. In our case Lorentz factors $\Gamma_2 - \Gamma_1 \sim \Gamma_2$ for these two components (Fender, Belloni, & Gallo 2004; Rees & Meszaros 1994). The wind deposits large amount of energy as \dot{m}_{wind} approaches \dot{m}_{accr} prior to the switching on of superluminal flare. GRS 1915+105 produces upto 1 Jy superluminal flares with apparent velocity, β_{app} in a range 1.2–1.7. It is an efficient internal shock scenario where not just velocity but total jet power has significantly increased (Fender, Belloni, & Gallo 2004). This view is further strengthened by the fact that Cyg X-3 can produce superluminal flares with flux density upto 15 Jy with $\beta_{app} \sim 0.69$ where the companion star can provide denser wind. The internal shock model can easily accommodate high jet power requirement $\geq 10^{38}$ ergs s $^{-1}$ (Fender et al. 1999) and can explain the shifting from thick to thin radio emission during superluminal flares (Kaiser, Sunyaev, & Spruit 2000).

Radio plateaux occur when \dot{m}_{accr} , as inferred from the X-ray flux, is very high and L_{bol} approaches L_{Edd} . As \dot{m}_{accr} rises, the accretion disk passes through an instability zone (prior to plateau state) and produces pre-plateau flares (see Figure 1). Thereafter, it enters in steady plateau state. At the end of the plateau state, changes in \dot{m}_{accr} again produce instabilities in the accretion disk which produce post-plateau flare (flare which produce superluminal flare) and the source comes out of plateau state. It may be noted here that a post-plateau flare may not always end plateau state but it may change the level of the plateau as is the case of superluminal flares on 1998 April 13 & 30 (plateau radio flux 91 mJy (highest flux in Table 1)). The instabilities in the accretion disk may be triggered by either a change in \dot{m}_{accr}

or by some adjustment among different accretion flows (Yadav et al. 1999). This view is supported by the finding that certain X-ray variability classes are observed preferably before and after the plateaux (low hard state) (Naik et al. 2002).

Our results presented here suggest only three types of radio emission in GRS 1915+105 ; (1) radio emission during the steady plateau state with β in a range 0.1–0.4 (steady X-ray properties), (2) oscillations or discrete baby jets with $\beta \sim 1$ (state transition in X-rays), and (3) faint flares of 2–3 min durations with likely low β (hard X-ray spectrum changes but no state transition (Rothstein, Eikenberry, & Matthews 2005)). The superluminal flares are the consequences of class 1 & class 2 radio emissions when occur in this order (but not in the reverse order). Our description of superluminal flares here can explain why axis of superluminal flares differs by $\leq 12^\circ$ from the axis of AU scale compact jets (Dhawan, Mirabel, & Rodriguez 2000). The wind is radiation-driven and is expected to originate from the inner part of the accretion disk while the compact jets are most likely to originate from the outer corona. The phase lag between the hard and soft X-ray photons in GRS 1915+105 changes sign during the plateau state and produce complex behavior (Muno et al. 2001). Varniere (2005) has suggested that anything located inside the inner radius of the accretion disk (in our case wind) that can absorb a small part of soft X-ray flux can explain the changing of sign of the lag and its complex behavior during the plateau state. Other consequences of our results is that one would not expect oscillations/baby jet type of IR & radio emission in Cyg X-3 (not observed so far (Dhawan, Mirabel, & Rodriguez 2000)) as has been observed in GRS 1915+105 (Mirabel et al. 1998; Eikenberry et al. 1998; Ishwara-Chandra, Yadav, & Pramesh Rao 2002). Any discrete jet (including oscillations) should produce internal shock as wind from the companion is always present in the case of Cyg X-3 and therefore, such jet would always end up producing a superluminal jet with thin radio emission.

The physics in all the systems dominated by black holes is essentially the same and therefore, it is always tempting to compare microquasars with massive extragalactic AGNs and quasars. The correlation between radio and X-ray luminosity during the low hard state (Gallo, Fender, & Pooley 2003) can be extended to the AGNs by including a black hole mass term (Merloni, Heinz, & di Matteo 2003; Falcke, Koerding, & Markoff 2004). Therefore the steady jets in microquasars during radio plateaux are directly comparable with those in AGNs. Marscher et al. (2002) have claimed to observe oscillation radio jet ($\sim 1/\text{year}$) in AGN 3C120. They related these radio jets to superluminal ejection events which can be understood in the frame work of the model discussed here (if we assume the presence of warm absorber). The results discussed in this paper suggest the propagation of shock wave to produce the superluminal jets in microquasars, a interpretation usually favoured for jets in extragalactic systems. It is shown recently that the jets in microquasars are as relativistic as AGN jets provided the jets in microquasars are not confined and the derived opening angles are solely due to the

relativistic effect (Miller-Jones, Fender, & Naker 2006; Gopal-Krishna, Dhurde, & Wiita 2004). It is natural to associate (though disputed!) the radio loud and radio quiet dichotomy observed in AGN with jet-producing low hard state and non-jet-producing high soft state in microquasars (Maccarone, Gallo, & Fender 2003). The PDS of luminous narrow line Seyfert 1 AGNs appears to be similar to the one observed during the high soft state in microquasars while the PDS of the low luminosity AGNs is similar to the one observed during the low hard state in microquasars (McHardy et al. 2004; Markowitz & Uttley 2005). Shocks are related to the most energetic processes in the universe (Gamma ray bursts, large superluminal jets in microquasars and AGNs) and microquasars provide a great opportunity to study them under the best possible conditions within reasonable time.

4. CONCLUSIONS

We present for the first time clear evidences of direct connection between the accretion disk during plateaux and the following superluminal radio flares. We find that the \dot{m}_{accr} , as inferred from the X-ray flux, is very high during the radio plateaux and L_{bol} approaches L_{Edd} . We suggest that such hot accretion disk during the radio plateaux always accompany with radiation-driven wind. The internal shock forms in the previously generated slowly moving wind from the accretion disk with $\beta \leq 0.01$ as the fast moving discrete jet with $\beta \sim 1$ catches up and interacts with it. Both the components; slow moving wind and fast moving jet are related to the accretion disk during plateau state and the strength & speed of these two should determine the power of the internal shock. In GRS 1915+105, it is a efficient internal shock scenario where not just velocity but total jet power has significantly increased. The superluminal flares have steep radio spectrum and are observed at large distances from the compact object (≥ 240 AU). The profile of the superluminal radio flares can be described as fast rise and exponential decay (FRED).

The other radio flares observed in GRS 1915+105 include the persistent radio emission during the plateaux (20–160 mJy), the radio oscillations & discrete radio flares (5–150 mJy) and the preplateau radio flares (50–360 mJy). All of these are observed close to the compact object (< 200 AU) and have flat or inverted radio spectra. During the radio plateaux, both the radio flare and the accretion disk are in steady state (outflow and inflow in the accretion disk are in equilibrium) and a tight correlation is observed between the radio luminosity and the X-ray luminosity as discussed earlier. The IR & radio oscillations (5–150) are periodic ejections of adiabatically expanding self absorbing synchrotron clouds (Mirabel et al. 1998; Ishwara-Chandra, Yadav, & Pramesh Rao 2002). The IR flux suggests that the ejected matter decouples from the accretion disk at the time of the spike in the X-rays (Eikenberry et al. 1998). The preplateau radio flares (50–360 mJy) are discrete ejections which are closely spaced in time and hence produce overlapped radio flares. The preplateau flares have been modeled as adiabatically expanding self absorbing clouds ejected from the accretion disk which explain reasonably well all the available observed data of time delay for radio emission at lower

frequency (Ishwara-Chandra, Yadav, & Pramesh Rao 2002). It is widely believed that it is the coronal material and not the disk material which is ejected prior to radio flares (Rau & Greiner 2003; Vadawale et al. 2003; Fender, Belloni, & Gallo 2004; Rothstein, Eikenberry, & Matthews 2005). During oscillations/discrete flares and the preplateau flares, the coronal mass ejections affect the hard X-ray component (Compton component) either partly or completely (state change) (outflow and inflow are not in equilibrium in this case unlike during the plateaux).

Author thanks the referee for his/her useful comments which have greatly improved the presentation of the paper and will enhance its impact. Author also thanks RXTE PCA/HEXTE and NSF-NRAO-NASA Green Bank Interferometer teams for making their data publicly available. The Green Bank Interferometer is a facility of the National Science Foundation operated by the NRAO in support of NASA High Energy Astrophysics programs.

REFERENCES

- Belloni, T., Mendez, M., King, A. R., et al. 1997, *ApJ*, 488, L109
 Belloni, T., Klein-Wolt, M., Mendez, M., et al. 2000, *A&A*, 355, 271
 Dame, T. M., Hartmann, D. & Thaddeus, P. 2001, *ApJ*, 547, 792
 Dhawan, V., Muno, M. P., Remillard, R., et al. 2003 preprint.
 Dhawan, V., Mirabel, I. F. & Rodriguez, L. F. 2000, *ApJ*, 543, 373
 Dickey, J. M. & Lockman, F. J. 1990, *ARA&A*, 28, 215
 Chris, Done & Kubota, Aya 2005, *astro-ph/0511030*
 Eikenberry, S. S., Matthews, K., Morgan, E. H., et al. 1998, *ApJ*, 494, L61
 Eikenberry, S. S., Matthews, K., Muno, M. et al. 2000, *ApJ*, 532, L33
 Elvis, Martin 2000, *ApJ*, 545, 63
 Falcke, H., Koerding, E. & Markoff, S. 2004, *A&A*, 414, 895
 Fender, R. P. 2001, *MNRAS*, 322, 31
 Fender, R. P. & Belloni, T. M. 2004, *ARA&A*, 42, 317
 Fender, R. P., Belloni, T. M. & Gallo, E. 2004, *MNRAS*, 355, 1105
 Fender, R. P., Garrington, S. T., McKay, D. J. et al. 1999, *MNRAS*, 304, 865
 Fuchs, Y., Mirabel, I. F. & Claret, A. 2003, *A&A*, 404, 1011
 Fuchs, Y., Rodriguez, J., Mirabel, I. F. et al. 2003, *A&A*, 409, L35
 Gallo, E., Fender, R. P., & Pooley, G. G. 2003, *MNRAS*, 344, 60
 Gopal-Krishna, Dhurde, S., & Wiita, P. J. 2004, *ApJ*, 614, L81
 Greiner, J., Cuby, J. G., & McCaughrean, M. J. 2001, *Nature*, 414, 522
 Hjellming, R. M., & Rupen, M. P. 1995, *Nature*, 375, 464
 Ishwara-Chandra, C. H., Yadav, J. S., & Pramesh Rao, A. 2002, *A&A*, 388, L33
 Kaiser, C. R., Sunyaev, R. & Spruit, H. C. 2000, *A&A*, 356, 975
 Klein-Wolt, M., Fender, R. P., Pooley, G. G., et al. 2002, *MNRAS*, 331, 745
 Koch-Miramond, L., Abraham, P., Fuchs, Y., et al. 2002, *A&A*, 396, 877
 Kotani, T., Ebisawa, K., Dotani, T., et al. 2000, *ApJ*, 539, 413
 Lee, J. C., Reynolds, C. S., Remillard, R., et al. 2002, *ApJ*, 567, 1102
 Maccarone, T., Gallo, E., & Fender, R. P. 2003, *MNRAS*, 345, L19
 Markowitz, A., & Uttley, P. 2005, *ApJ*, 625, L39
 Marscher, A. P., Jorstad, S. G., Gomez, J. L., et al. 2002, *Nature*, 417, 625
 McHardy, I. M., et al. 2004, *MNRAS*, 348, 783
 Meier, D. L. 2005, *AP&SS*, 300, 55
 Merloni, A., Heinz, S. & di Matteo, T. 2003, *MNRAS*, 345, 1057
 Migliari, S. & Belloni, T. 2003, *A&A*, 404, 283
 Miller, J. M., Raymond, J., Fabian, A. C., et al. 2004, *ApJ*, 601, 450
 Miller-Jones, J. C. A., Fender, R. P. & Naker, E. 2006, *MNRAS*, in Press
 Mirabel, I. F., & Rodriguez, L. F. 1994, *Nature*, 371, 46
 Mirabel, I. F., Dhawan, V., Chaty, S. et al. 1998, *A&A*, 330, L9
 Morgan, E. H., Remillard, R. A. & Greiner, J. 1997, *ApJ*, 482, 1010
 Muno, M. P., Morgan, E. H. & Remillard, R. A. 1999, *ApJ*, 527, 321
 Muno, M. P., Remillard, R. A., Morgan, E. H., et al. 2001, *ApJ*, 556, 515
 Naik, S., Agrawal, P. C., Rao, A. R., et al. 2002, *MNRAS*, 330, 487
 Ogley, R. N., Burnell, S. J. B. & Fender, R. P. 2001, *MNRAS*, 322, 177
 Orosz, J. A., Kuulkers, E., van der Klis, M. 2001, *ApJ*, 555, 489
 Pooley, G. G. & Fender, R. P. 1997, *MNRAS*, 292, 925
 Rao, A. R., Naik, S., Vadawale, S. V. & Chakrabarti, S. K. 2000, *A&A*, 360, L25
 Rao, A. R., Yadav, J. S. & Paul, B. 2000, *ApJ*, 544, 433
 Rau, A., & Greiner, J. 2003, *A&A*, 397, 711
 Remillard, R. A. 2005 *astro-ph/0504129*
 Rees, M. J., & Meszaros, P. 1994, *ApJ*, 430, L93
 Ribo, M., Dhawan, V. & Mirabel, I. F. 2004, *Proc. 7th European VLBI network symposium*, p. 111
 Rothstein, D. M., Eikenberry, S. S. & Matthews, K. 2005, *ApJ*, 626, 991
 Shaposhnikov, N., & Titarchuk, L. 2006, *ApJ*, in press
 Vadawale, S. V., Rao, A. R. & Naik, S. 2002, in *Proc. 4th Microquasar Workshop*, ed. P. Durouchoux, Y. Fuchs & J. Rodriguez, 338
 Vadawale, S. V., Rao, A. R., Naik, S., Yadav, J. S., et al. 2003, *ApJ*, 597, 1023
 Ueda, Y., Inoue, H., Tanaka, Y., Ebisawa, K., et al. 1998, *ApJ*, 492, 782 (erratum 500, 1069)
 Ueda, Y., Yamaoka, K., Sanchez-Fernandez, C., et al. 2002, *ApJ*, 571, 918
 Varniere, P. 2005, *A&A*, 434, L5
 Wu, K., Soria, R., Campbell-Wilson, D., et al. 2002, *ApJ*, 565, 1161
 Yadav, J. S., Rao, A. R., Agrawal, P. C., et al. 1999, *ApJ*, 517, 935
 Yadav, J. S. 2001, *ApJ*, 548, 876
 Yadav, J. S., Ishwara-Chandra, C. H., Pramesh Rao, A., & Pooley, G. G. 2003, in *Proc. 4th Microquasar Workshop*, ed. P. Durouchoux, Y. Fuchs & J. Rodriguez, 305
 Yadav, J. S., 2006, under publication in *ApJ Letters*

TABLE 1
ALL SELECTED SUPERLUMINAL RADIO FLARES AND THEIR PROPERTIES (SEE TEXT FOR DETAILS). X-RAY PROPERTIES FROM RXTE
PCA/HEXTE DATA DURING PRECEDING RADIO PLATEAU.

Superluminal Radio Flare Properties					Associated Preceding Plateau Properties					
MJD/ Date	Peak Flux (mJy)	Rise Time (day)	Decay Time constant (days)	Radio Flux ^a (Jy.day)	GBI Flux (mJy)	ASM Flux (c/s)	Date of RXTE Obser.	QPO Freq. (Hz)	Total X-ray Flux ^b	N _H (10 ²² cm ⁻²)
50750/1997 Oct 30	550	<0.6	3.16 ^{+0.07} _{-0.09}	2.20 [#]	47.3	35.9	1997 Oct. 25	1.88	2.04	13.27 ^{+0.66} _{-0.91}
50916/1998 Apr 13	920	<0.8	4.02 ^{+0.36} _{-0.33}	3.04	91.0	48.2	1998 Apr. 11	1.60	2.42	14.95 ^{+0.82} _{-0.65}
50933/1998 Apr 30	580	<0.9	3.98 ^{+0.13} _{-0.13}	3.02	91.0	44.9	1998 Apr. 28	1.41	2.34	13.55 ^{+0.78} _{-0.31}
50967/1998 Jun 03	710	0.3	2.82 ^{+0.48} _{-0.28}	2.15	56.2	36.5	1998 May 31	1.76	2.14	12.99 ^{+0.81} _{-0.32}
51204/1999 Jan 30	340	0.25	1.12 ^{+0.03} _{-0.05}	0.36	27.8	33.8	1999 Jan. 24	2.55	1.84	11.19 ^{+0.92} _{-0.95}
51337/1999 Jun 08	490	<0.7	2.67 ^{+0.22} _{-0.16}	1.58	45.5	35.2	1999 Jun. 03	1.77	1.98	12.43 ^{+0.95} _{-1.15}
51535/1999 Dec 23	510	<0.8	2.67 ^{+0.12} _{-0.14}	1.75 [#]	51.3	38.9	1999 Dec. 21	2.12	2.23	13.61 ^{+1.17} _{-0.94}
52105/2001 Jul 16 ^c	210	<0.7	1.77 ^{+0.20} _{-0.20}	0.62 [#]	20.0	30.0	2001 Jul. 11	2.40	1.75	10.60 ^{+0.77} _{-0.40}

- a:** Integrated flux is obtained by fitting an exponential function to the flare profile and integrating the function over duration of 3×decay time constant. Typical errors are ±0.05 (larger error (0.15–3.0) when marked “#” due to large gap in GBI radio data or due to contribution by additional radio flare)
b: Integrated 3–150 keV X-ray flux in 10⁻⁸ ergs cm⁻² s⁻¹
c: VLBA radio data (see text for details)

TABLE 2
BEST FIT SPECTRAL PARAMETERS FOR THE X-RAY OBSERVATIONS PRIOR TO THE RADIO FLARES SHOWN IN TABLE 1.

Day of RXTE obs.	3 – 150 keV flux (in 10 ⁻⁸ ergs cm ⁻² s ⁻¹)				kT _{in} keV	kT _e keV	τ	Γ	R _{in} ^a km	χ _ν ² (dof)
	F _{total}	F _{dbb}	F _{ctt}	F _{pow}						
1997 Oct. 25	2.04	0.20	0.75	0.97	0.50 ^{+0.02} _{-0.01}	5.50 ^{+0.16} _{-0.23}	7.7 ^{+0.8} _{-0.6}	2.47 ^{+0.30} _{-0.03}	748.1	1.40(74)
1998 Apr. 11	2.42	0.29	0.93	1.05	0.46 ^{+0.01} _{-0.01}	4.04 ^{+0.13} _{-0.30}	9.7 ^{+0.9} _{-0.8}	2.97 ^{+0.09} _{-0.03}	1392.4	0.83(94)
1998 Apr. 28	2.34	0.29	1.04	0.85	0.50 ^{+0.01} _{-0.01}	4.18 ^{+0.15} _{-0.22}	8.8 ^{+1.0} _{-0.4}	2.50 ^{+0.12} _{-0.19}	831.4	1.43(94)
1998 May 31	2.14	0.25	0.85	0.91	0.51 ^{+0.01} _{-0.01}	4.96 ^{+0.22} _{-0.51}	8.5 ^{+1.0} _{-0.7}	2.69 ^{+0.24} _{-0.06}	741.7	0.93(94)
1999 Jan. 24	1.84	0.128	0.60	1.0	0.57 ^{+0.01} _{-0.01}	7.00 ^{+0.22} _{-0.60}	4.2 ^{+1.9} _{-0.3}	2.39 ^{+0.14} _{-0.09}	297.0	1.15(93)
1999 Jun. 03	1.98	0.23	0.73	0.92	0.51 ^{+0.01} _{-0.01}	5.98 ^{+0.80} _{-0.60}	7.7 ^{+0.7} _{-1.3}	2.52 ^{+0.23} _{-0.12}	660.9	1.16(88)
1999 Dec. 21	2.23	0.25	0.71	1.16	0.48 ^{+0.02} _{-0.01}	5.25 ^{+0.76} _{-0.39}	8.3 ^{+1.1} _{-2.2}	2.82 ^{+0.03} _{-0.07}	981.3	0.81(88)
2001 Jul. 11	1.75	0.13	0.50	0.95	0.54 ^{+0.02} _{-0.01}	6.99 ^{+0.36} _{-0.59}	7.1 ^{+0.5} _{-1.5}	2.39 ^{+0.03} _{-0.07}	354.3	0.98(87)

^a: R_{in} derived assuming distance D = 12.5 kpc and inclination angle, θ = 70°

: associated best fit values of N_H is shown in Table 1